THE DYNAMIC PHENOMENA ARROUND OF TRANSITION TO WHEELSET SLIP AT LOCOMOTIVE DRIVE WITH JOINT SHAFT INSIDE HOLLOW ROTOR

Michael Lata

michael.lata@upce.cz

Department of Transport Means, The Jan Perner Transport Faculty, University of Pardubice, Studentska 95, 532 10 Pardubice, CZECH REPUBLIC

Key words: *wheelset drive, transitional dynamics action, simulation calculation*

Summary: *This paper shortly shows dynamics torsion system simulation of railway drive vehicle. The cooperation cases of adhesive characteristics with drive motor characteristics behind downgrade adhesive conditions they are simulation and influence on all system dynamics is analyzing.*

The formulation of problem

The objective of simulation calculations is the identification of dynamic transitional actions at torsion wheelset drive system. The significant influence of the adhesive characteristics and drive motor moment characteristics is predicted. The solution considered of the simplified dynamic model making, make-up the equations of motion, numeric method programming for time simulation calculations, nonlinear adhesion model implementation, driving moment model implementation.

1. Model of wheelset drive with joint shaft inside the hollow rotor

The electric locomotive Skoda class 150 is DC locomotive for supply voltage 3000 V, with maximum power 3 MW, maximum speed 140 km/h, with DC series motor, regulated by resistances. The drive of wheelset is by joint shaft inside hollow rotor of tractive motor. Stator is stationary mounted at bogie frame. Gearbox is beared at the axle and hang at bogie frame.
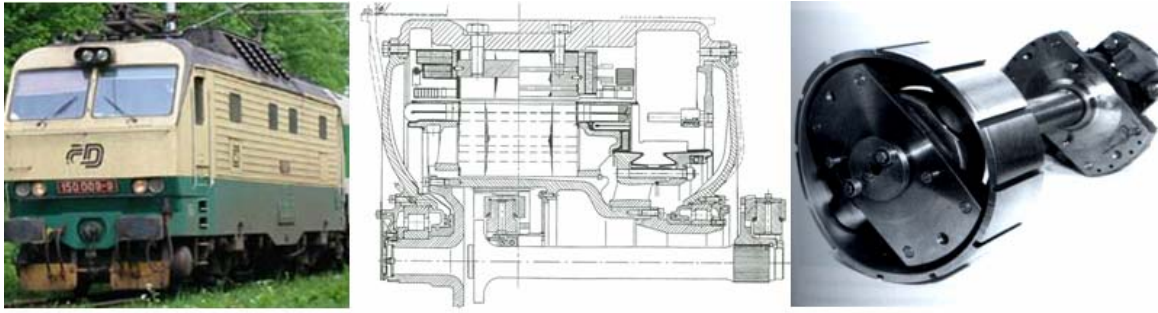
Fig. 1 Electric locomotive SKODA with joint shaft inside the hollow rotor and detail section
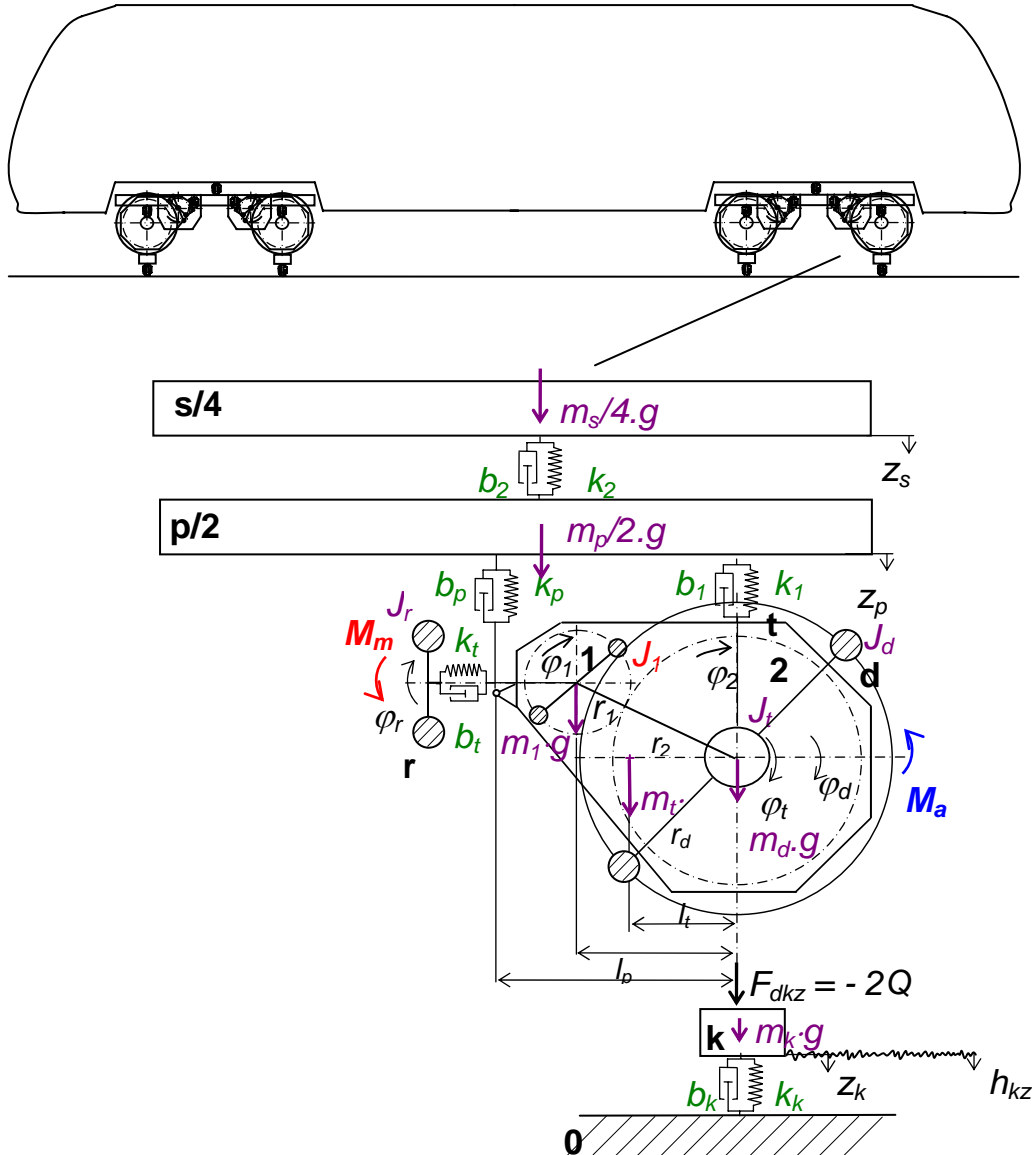

Fig. 2 Model of wheelset drive with joint shaft inside the hollow rotor – locomotive Skoda 150

The equation of motions was build by Lagrange 2th type equation method. For separately masses and coordinates has this form:

The ¼ mass of body case (coordinate z_s):

$$\frac{m_s}{4} \cdot \ddot{z}_s + b_2 \cdot \left(\dot{z}_s - \dot{z}_p\right) + k_2 \cdot \left(z_s - z_p\right) = \frac{m_s}{4} \cdot g$$

The ½ mass of bogie (coordinate z_p):

$$\frac{m_p}{2} \cdot \ddot{z}_p + b_1 \cdot \left(\dot{z}_p - \dot{z}_k \right) - b_2 \cdot \left(\dot{z}_s - \dot{z}_p \right) + b_p \cdot \left(\dot{z}_p - \dot{z}_k + \dot{\varphi}_t \cdot l_p \right)$$

$$+ k_1 \cdot \left(z_p - z_k \right) - k_2 \cdot \left(z_s - z_p \right) + k_p \cdot \left(z_p - z_k + \varphi_t \cdot l_p \right) = \frac{m_p}{2} \cdot g$$

Wheelset and reduced mass of rail and gear box (coordinate z_k):

$$\left(m_d + m_k + m_t + m_1 \right) \cdot \ddot{z}_k - \left(m_t \cdot l_t + m_1 \cdot l_1 \right) \cdot \ddot{\varphi}_t - b_1 \cdot \left(\dot{z}_p - \dot{z}_k \right) - b_p \cdot \left(\dot{z}_p - \dot{z}_k + l_p \cdot \dot{\varphi}_t \right)$$

$$+ b_k \cdot \dot{z}_k - k_1 \cdot \left(z_p - z_k \right) - k_p \cdot \left(z_p - z_k + l_p \cdot \varphi_t \right) + k_k \cdot z_k = \left(m_d + m_k + m_t + m_1 \right) \cdot g$$

Rotor (coordinate φ_r):

$$J_r \cdot \ddot{\varphi}_r + b_t \cdot \left[\dot{\varphi}_r - \left(1 + \frac{r_2}{r_1} \right) \cdot \dot{\varphi}_t + \frac{r_2}{r_1} \cdot \dot{\varphi}_d \right] + k_t \cdot \left[\varphi_r - \left(1 + \frac{r_2}{r_1} \right) \cdot \varphi_t + \frac{r_2}{r_1} \cdot \varphi_d \right] = -M_m$$

Gear box (coordinate φ_t):

$$\left[J_t + J_1 \cdot \left(1 + \frac{r_2}{r_1} \right)^2 + m_t \cdot l_t^2 + m_1 \cdot l_1^2 \right] \cdot \ddot{\varphi}_t - J_1 \cdot \left(1 + \frac{r_2}{r_1} \right) \cdot \frac{r_2}{r_1} \cdot \ddot{\varphi}_d -$$

$$- \left(m_t \cdot l_t^2 + m_1 \cdot l_1^2 \right) \cdot \ddot{z}_k + b_p \cdot \left(\dot{z}_p + l_p \cdot \dot{\varphi}_t - \dot{z}_k \right) \cdot l_p$$

$$- b_t \cdot \left[\dot{\varphi}_r - \left(1 + \frac{r_2}{r_1} \right) \cdot \dot{\varphi}_t + \frac{r_2}{r_1} \cdot \dot{\varphi}_d \right] \cdot \left(1 + \frac{r_2}{r_1} \right) + k_p \cdot \left(z_p + l_p \cdot \varphi_t - z_k \right) \cdot l_p$$

$$- k_t \cdot \left[\varphi_r - \left(1 + \frac{r_2}{r_1} \right) \cdot \varphi_t + \frac{r_2}{r_1} \cdot \varphi_d \right] \cdot \left(1 + \frac{r_2}{r_1} \right) = - \left(m_t \cdot l_t + m_1 \cdot l_1 \right) \cdot g$$

Wheelset (coordinate φ_d):

$$\left[J_d + J_1 \cdot \left(\frac{r_2}{r_1} \right)^2 \right] \cdot \ddot{\varphi}_d - J_1 \cdot \frac{r_2}{r_1} \cdot \left(1 + \frac{r_2}{r_1} \right) \cdot \ddot{\varphi}_t + b_t \cdot \frac{r_2}{r_1} \cdot \left(\dot{\varphi}_r - \left(1 + \frac{r_2}{r_1} \right) \dot{\varphi}_t + \frac{r_2}{r_1} \cdot \dot{\varphi}_d \right)$$

$$+ k_t \cdot \frac{r_2}{r_1} \cdot \left(\varphi_r - \left(1 + \frac{r_2}{r_1} \right) \varphi_t + \frac{r_2}{r_1} \cdot \varphi_d \right) = -M_a$$

For simulation calcullation and programming the numerical solver by final differences method is necessary of transform these equations to reduced shape, according to Newton´s notice form as:

$$\ddot{z}_j = \frac{\sum_{k=1}^{n} F_k}{m_j} \text{, resp. } \ddot{\varphi}_j = \frac{\sum_{k=1}^{n} M_k}{J_j} \text{ for rotation degrees of freedom.}$$

The forces and moments of bindings, deformation of bindings and velocities of deformation of bindings are computed separatelly.

The adhesion moment function between wheelset and rail and it´s given by tangencial forces that function at wheel perimeter. We ask functional dependence of angular speed of wheelset $M_a = f(\dot{\varphi}_d)$.

Tangencial forces between wheels and rails go out from so-called adhesion model, or adhesion mechanism. There is complicated phenomenon and is solwed

many authors how exact, so experimentally. The basic is relationship between normal force Q, tangential force T and adhesion coefficient μ is $T = Q \cdot \mu$.

The adhesive mechanism, using at these thorsional model, make use of theory of [1] and experimantal work of [2]. The distribution of stress don´t ellipsoid, according to Hertz contact theory, but section of the ball. The stress distribution is composite from 2 bodies: section of roller V_1 and section of ball V_2.
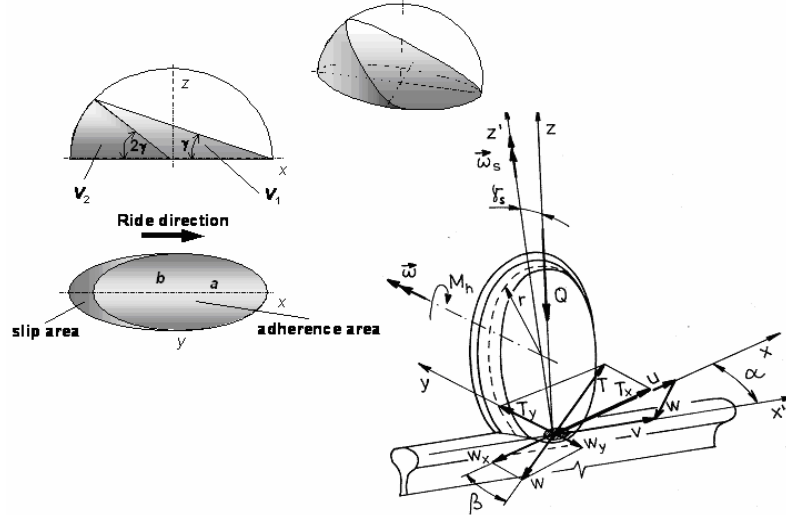

Fig. 3 Illustration of principle of the adhesive mechanism

Volumes:

$$V_1 = \frac{1}{2} \sin(2\gamma) \int_{-a}^{a} x^2 \, dw = \frac{1}{2} \sin(2\gamma) \int_{-a}^{a} \left(a^2 - w^2 \right) dw = \frac{4}{3} a^3 \, \sin\gamma \, \cos\gamma$$

$$V_2 = \frac{4}{3} \pi a^3 \frac{2\gamma}{2\pi} = \frac{4}{3} a^3 \gamma$$

General volume:

$$V = V_1 + V_2 = \frac{4}{3} a^3 \left(\sin\gamma \, \cos\gamma + \gamma \right) = \frac{4}{3} a^3 \left(\frac{tg\gamma}{1+tg^2\gamma} + \gamma \right) = \frac{4}{3} a^3 \left(\frac{\varepsilon}{1+\varepsilon^2} + arctg\,\varepsilon \right)$$

Slip velocities (α is strike angel):

$$w_x = r \cdot \omega - v \cdot \cos\alpha \; ; \; w_y = v \cdot \sin\alpha \; ; \; w = \sqrt{w_x^2 + w_y^2}$$

Relative creeps:

$$s_x = \frac{w_x}{v} \; ; \qquad s_y = \frac{w_y}{v} \; ; \qquad s = \sqrt{s_x^2 + s_y^2}$$

Tangencial forces:

$$T_x = Q \cdot \mu_x = Q \cdot \mu \cdot \frac{s_x}{s} \; ; \qquad T_y = Q \cdot \mu_y = Q \cdot \mu \cdot \frac{s_y}{s} \; ; \qquad T = \sqrt{T_x^2 + T_y^2}$$

Maximum tangencial stress:

$$\tau_m = p_m \cdot f$$

Maximum normal press:

$$p_m = \frac{3}{2} \cdot \frac{Q}{\pi \cdot a \cdot b}$$

Tangencial force:

$$T = \iint_L \tau_{xy} \, dx dy = \tau_m \cdot \frac{1}{a} \cdot \frac{b}{a} \cdot V = \frac{3}{2} \cdot \frac{Q}{\pi \cdot a \cdot b} \cdot f \cdot \frac{b}{a^2} \cdot V = \frac{3}{2} \cdot \frac{Q \cdot b}{\pi \cdot a^3} \cdot f \cdot V = Q \cdot \mu$$

Adhesion coefficient:

$$\mu = \frac{T}{Q} = \frac{\dfrac{3}{2} \cdot \dfrac{Q \cdot b}{\pi \cdot a^3} \cdot f \cdot V}{Q} = \frac{3}{2} \cdot \frac{b}{\pi \cdot a^3} \cdot f \cdot V =$$

$$= \frac{3}{2} \cdot \frac{b}{\pi \cdot a^3} \cdot f \cdot \frac{4}{3} a^3 \left(\frac{\varepsilon}{1+\varepsilon^2} + arctg\varepsilon \right) = \frac{2}{\pi} \cdot f \cdot \left(\frac{\varepsilon}{1+\varepsilon^2} + arctg\varepsilon \right)$$

where: $\quad \varepsilon = tg\gamma = \dfrac{2}{3} \cdot \dfrac{\pi \cdot a^2 \cdot b \cdot K \cdot s}{Q \cdot f} = \dfrac{a \cdot K \cdot s}{\tau_m} = \dfrac{a \cdot K \cdot s}{p_m \cdot f} = \dfrac{s}{\rho \cdot f}$

Q …. vertical wheel force,

a ….. head half-axis of strike ellipses,

K …. constant of elasticity of wheel and rail surfaces, that has influence at characteristic slope. According to [1], [2] and according to prof. Polach – Research center Bombardier Transportation [3].

The slope of adherence zone of adhesion curve is possible computed from reffered model as:

$$c_{\mu s} = \frac{d\mu}{ds} = \frac{d\mu}{d\varepsilon} \cdot \frac{d\varepsilon}{ds} = \frac{8}{3} \cdot \frac{a^2 \cdot b \cdot K}{Q} \cdot \frac{1}{\left(1+\varepsilon^2\right)^2}$$

Interesting is coparison this model with Kalker´s theory [2]. The Kalker coefficient c_{11} has the same relation as the $c_{\mu s}$.
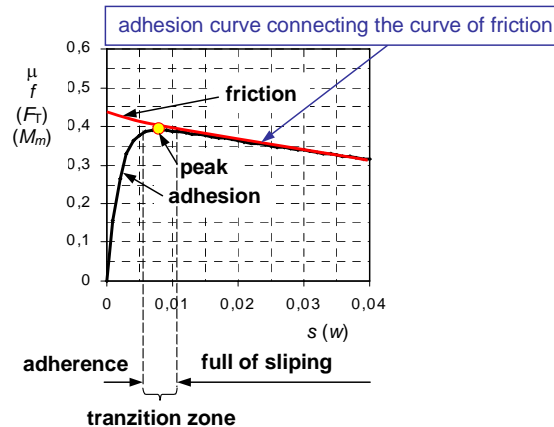

Fig. 4 Illustrative diagram of adhesion characteristic and its zones

Very significant at adhesion model is friction coefficient, that is not constant but dependence on creep velocity and adhesion conditions of adhesive surfaces.

The hypothesis about connection adhesion curve to friction curve was experimentaly validate many authors. The shape of friction curve we can approximation by function:

$$f = k_0 \cdot e^{-k_1 \cdot w} + k_2$$

The coefficients it can determine by experiments. The $k_0 = f_{max}$ maximum friction coefficient and coefficients k_1, k_2 represent qualite of adhesive surfaces. The similar relations present for example [3]. The coefficients for normal conditions was determine according by much experimental measureds and statistical evaluation according to [2] as:
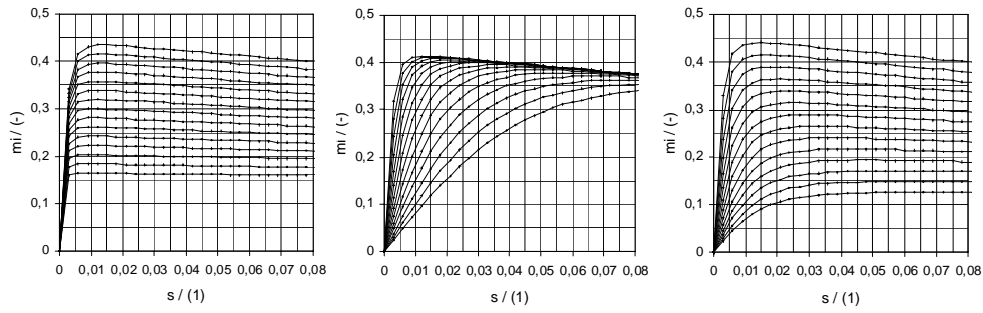
$$f = f_{max} \cdot e^{-0,75 \cdot w} + 0,125$$

Fig. 5   Courses of μ = f(s, fmax);   Courses of μ = f(s, K);   Courses of μ = f(s, fmax, K)
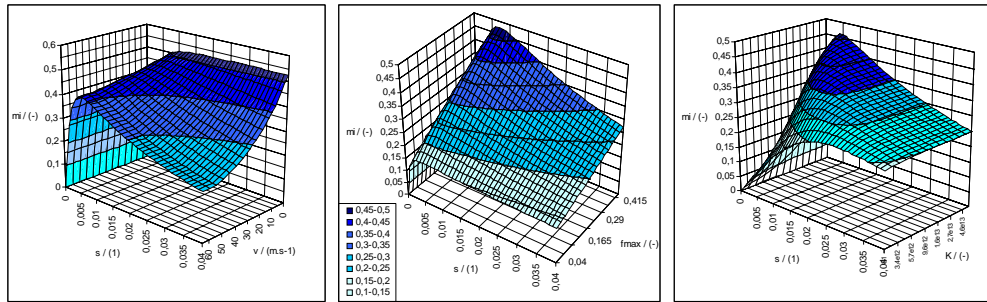

Fig. 6 The adhesive coefficient dependence on creep, speed, friction coefficient and steepness

Picture at *fig. 7a* shows working adhesive characteristics course of moment M_a. Depiction serves among others for checks of rightness algorithm function. Course is comparable with measured real characteristics shape (*fig. 7b*) according authors [2], [3] with typical unstability bifurcations on zone of slip.

The traction moment function at rotor of traction motor. We ask functional dependence at angular speed of rotor $M_m = f(\dot{\varphi}_r)$.

Traction moment is also dependence at electric parameters of motor, power supply and regulation. Model of electric part of drive is very dificult. For simply solving is possible using the linearization around of working point, because transitional actions orginate at relative small intervals of characteristics.
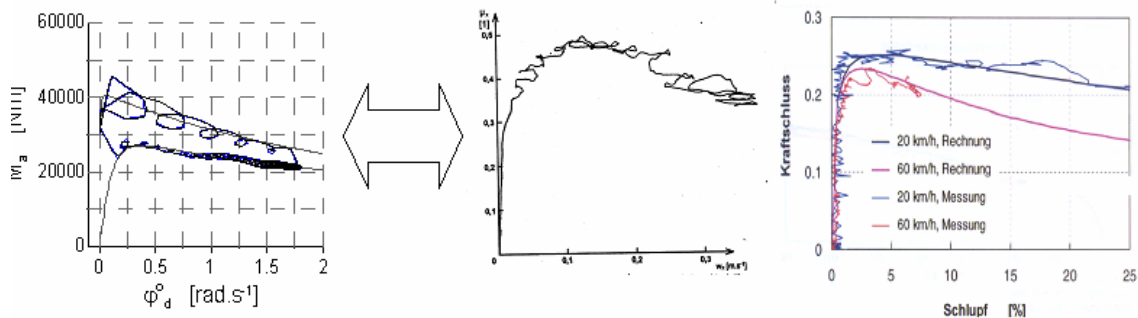

Fig. 7a Working characteristics of model   **Obr. 7b Shape of measured real characteristics**

The linear dependence is very real in case of direct-current motor with separately exciting. The constant k_1 signifies maximal value of drive moment and k_2 signifies the steepness. Moment characteristics of electric engine is:

$$M_m = k_1 - k_2 \cdot \dot{\varphi}_r$$

For precision simulations we must modelling real shape of characteristics and look at dependence of traction moment at electric parameters and electrical network dynamics.

The equation of circumference engagement of direct series motor are according to literature, for example [4] or [5]:

$$U = \sum R \cdot i + \sum L \cdot \frac{di}{dt} + k_\phi \cdot C_{ss} \cdot i \cdot \dot{\varphi}_r$$

$$M_m = k_\phi \cdot C_{ss} \cdot i^2$$

The adjustment of equation is necessery, so that we obtain the record of equation, formally the same with Newton´s form of equation of motion by reason of using numerical methods. We ask the dependence of elektromotor moment on rotor angular speed and electric parameters. The first equation will be after adjustment, that faces to use of the final differences method for numerical solution of time derivation we reduct to form:

$$U = \left(R_p + R_a + R_b\right) \cdot i_i + L_c \cdot \frac{i_{i-1} - i_{i-2}}{\Delta t} + k_\phi \cdot C_{ss} \cdot i_i \cdot \dot{\varphi}_r$$

From this equation we select current:

$$i_i = \frac{U - L_c \cdot \dfrac{i_{i-1} - i_{i-2}}{\Delta t}}{R_p + R_a + R_b + k_\phi \cdot C_{ss} \cdot \dot{\varphi}_r}$$

And introduce to equation for moment:

$$M_m = \frac{k_\phi \cdot C_{ss} \cdot \left(U - L_c \cdot \dfrac{i_{i-1} - i_{i-2}}{\Delta t}\right)^2}{\left(R_p + R_a + R_b + k_\phi \cdot C_{ss} \cdot \dot{\varphi}_r\right)}$$

The difference of current is introduced from last iteration step. The incorrectness is insignificant, because iteration time step is very small $\Delta t = 1.10 \div 5$s.

We can see, at *Fig. 9,* that around of working point, there is range of transitional dynamic action, the shape of characteristics approached to lines and we can linearize them.
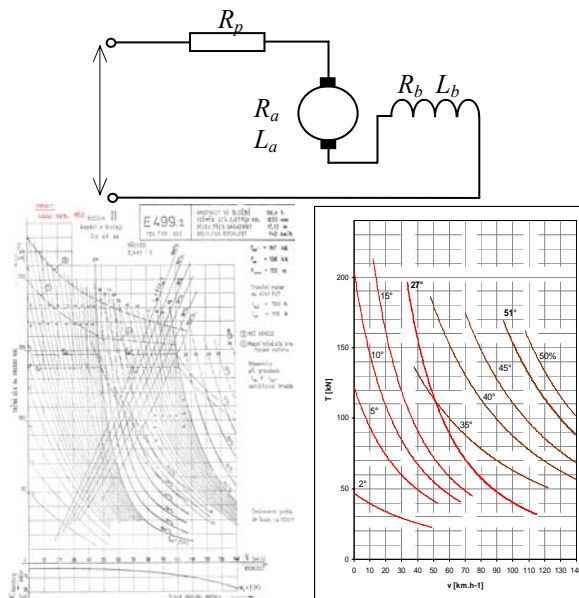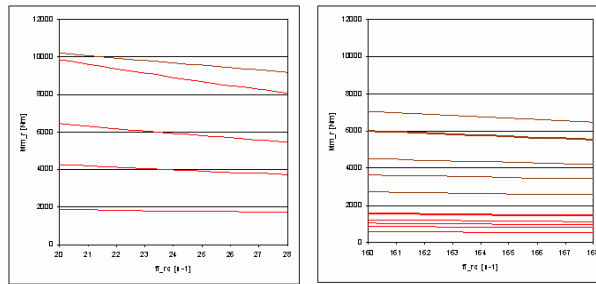

Fig. 8 The real tractive characteristisc and modeling courses electrical parameters for Skoda class 150 and traction motor Skoda 4-FXA7065

Fig. 9 Moment characteristics of one motor at rotor coordinates for the assumed range of simulated transitional actions

2. The transitional phenomena at wheelset torsional dynamics

At torsional driving system of railway driving vehicles exist the dynamic transitional process of mechanic oscillation. The dynamics transitional actions occure at these cases:

1) Influence of real vertical rail deviations on torsion dynamics – influence of kinematic bindings between vertical and torsional relative motions.

2) Cooperation cases of adhesive characteristics with drive motor characteristics behind downgrade adhesive conditions.

3) Cooperation cases of adhesive characteristics with drive motor characteristics behind course of transition between traction running and braking.

Now we can turn attention at a cooperation cases of adhesive characteristics with drive motor characteristics behind downgrade adhesive conditions. It is the base idea of transition process simulation: system work in work point. Change of adhesive characteristics is simulated at certain time interval. System begins change coordinates so, to stabilize (convergency) – or unstable (divergency) in new working point. Come to rise of self-excitation oscillating on negative part of adhesion curve. Next transition process can be simulated at return on original characteristics - return on original characteristics.
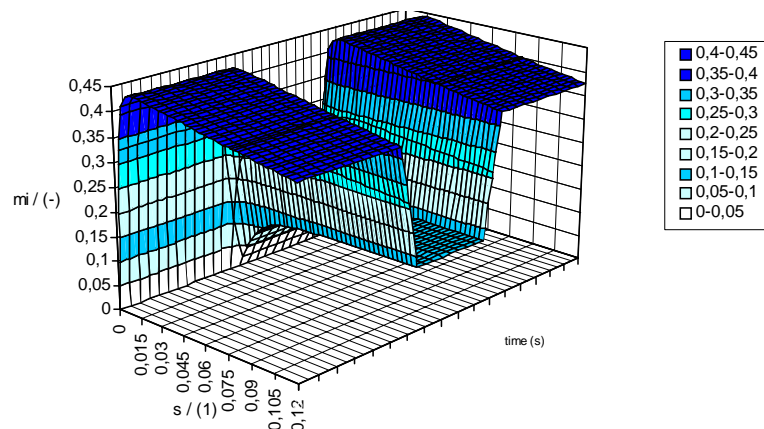
Fig. 10 The principle of time simulation of downgrade adhesion and return come back

Keynote of dynamic transitional action simulations of rise, continuation and extinction (handhold) wheelset slip consists in model cooperation of adhesive characteristics with drive motor characteristics. Characteristics oneself secant in the working point. Exist several case of characteristics cooperation. The next figures shows subcritical and supercritical curve cooperation.

UK-2.8

- Subcritical cooperation: Engine moment crossing new adhesive characteristics in her effective parts, or rise slip is handholded by downward branches of new characteristics.
- Critical cooperation: Engine moment curve is laying on the adhesion characteristic curve. It is limit condition.
- Supercritical cooperation: Drive motor torque characteristics has so small steepness, that lies over new adhesive characteristics and not crossing her. System behaviour depends for a short time, in that is of arose slip handhold by restoration of adhesive conditions. Depend on what, if is it before or under point, where engine graph cross original adhesive waveform. As far as restoration of adhesive conditions occurs before thereby point, is here surplus of adhesive moment - system slow and converge into stable condition. As far as with system gets behind this point, amplitudes trend henceforth growth.
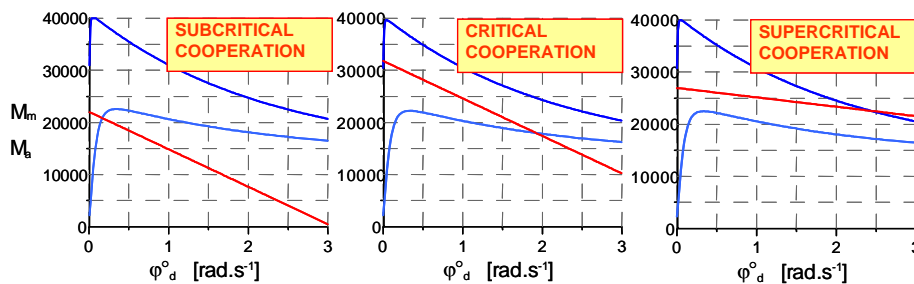

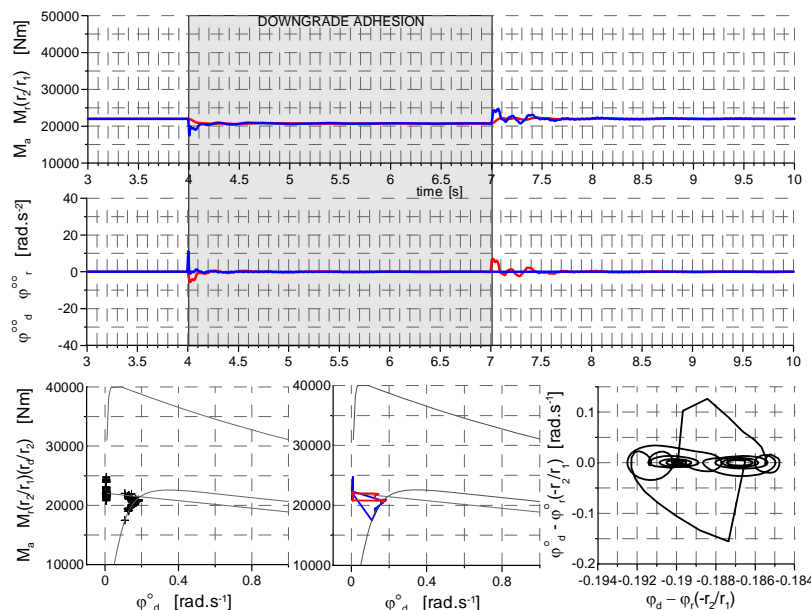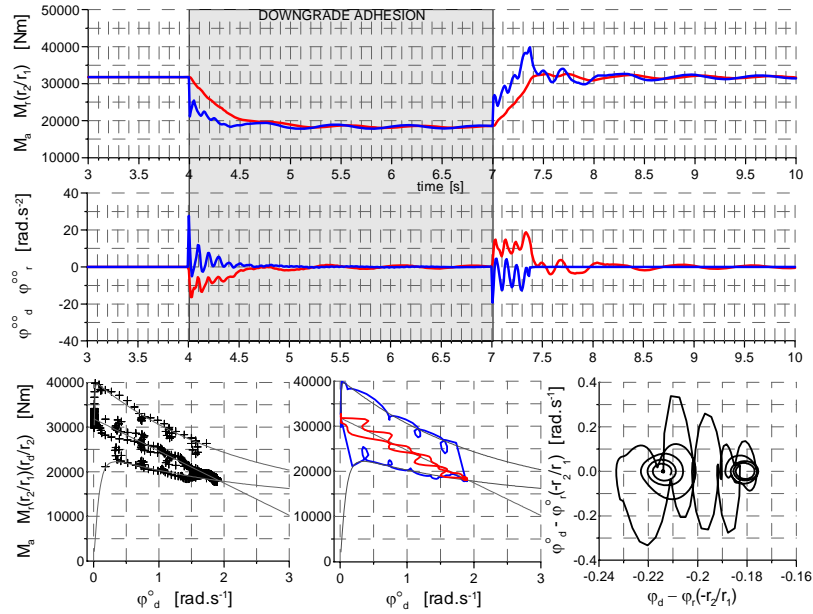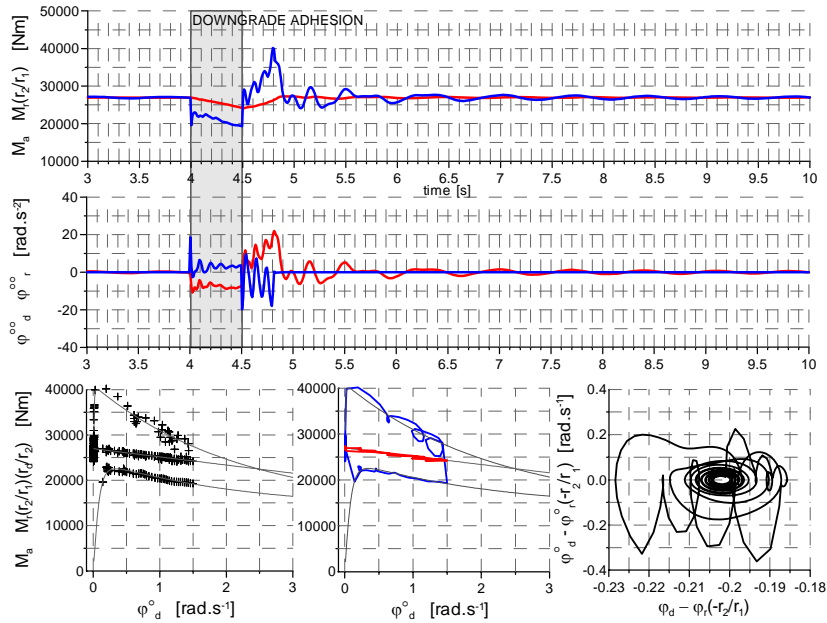**Fig. 11 Three states of characteristics cooperation**

Fig. 12 Subcritical cooperation – engine moment crossing new adhesive characteristics in her effective parts

Fig. 13 Subcritical cooperation – rise slip is handholded by downward branches of new adhesive characteristics


Fig. 14 Supercritical cooperation – 0,5s – before cross point - surplus of adhesive moment - system slow and converge into stable condition
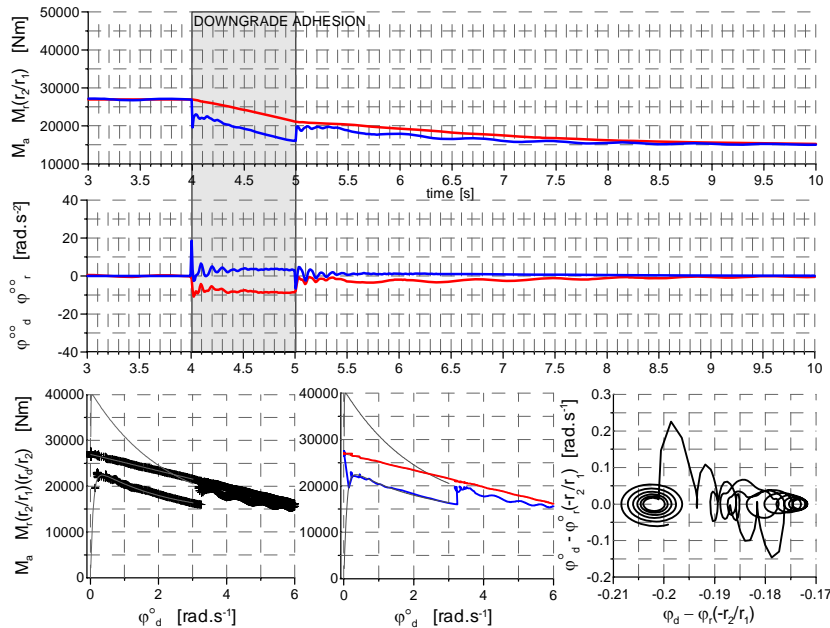
Fig. 15 Supercritical cooperation – 1s – system gets behind cross point - amplitudes trend henceforth growth

At case of transition between traction and motor braking for instantaneous value adhesion coefficient μ and friction coefficient f was using modification of friction coefficient form. The braking adhesion characteristics at section can have a special curve shape according to UIC. This shape could we modelling. The symetric shape of adhesion function was used.

Demonstration of simulation calculations: change of drive moment was design at simulation between 4th and 7th seconds. Return on original engine characteristics followed after 7th seconds. Two cases they are shown: decrease of driving moment on zeros ($M_m = 0$) and second case demonstrate the simulation of transition between traction and brake sections of adhesion characteristics.
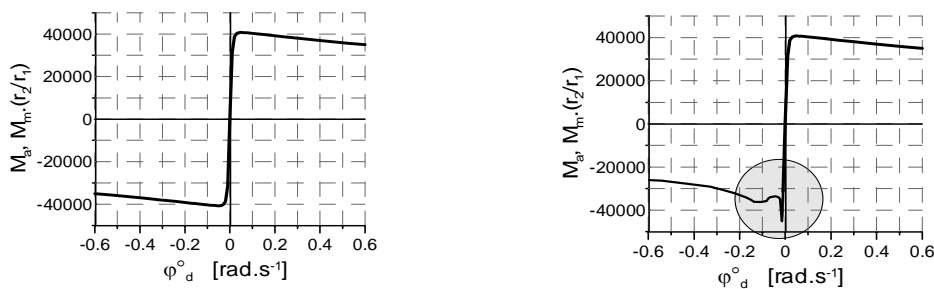
Fig. 16 Symetric characteristics traction braking and special shape according to UIC

Presuming with that clearance in torsional system have in these transitional modes considerable influence. There is clearances in gear and joint of cardan shaft. If the clearances at gear and at joint clutch is about 2 mm, then transformated angle clearances in axle axes is about 0,003 rad.

The simulation of decrease of driving moment on zeros ($M_m = 0$) was design as change of drive moment characteristics between 4th and 7th seconds of simulation calculation. The graphs shows a high frequency oscillating which follow by clearances in torsional system. The working characteristics of binding shows in right of this graph. At reality we can interpret it as a high frequency beats tooth of gear.
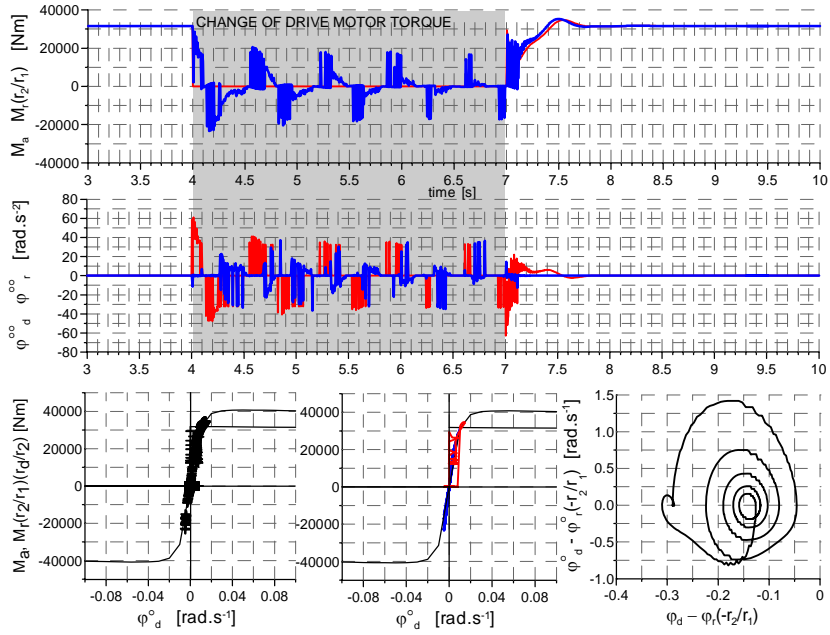
Fig. 17 Stop of traction moment function $M_m = 0$

At *fig. 19* we can see analysis of bifurcation of working points. The rotor coordinate after start of transitional process form traction to braking "ask" and converges the new stabil working point. After start of opposite transitional process from braking to traction it´s return to original working point.
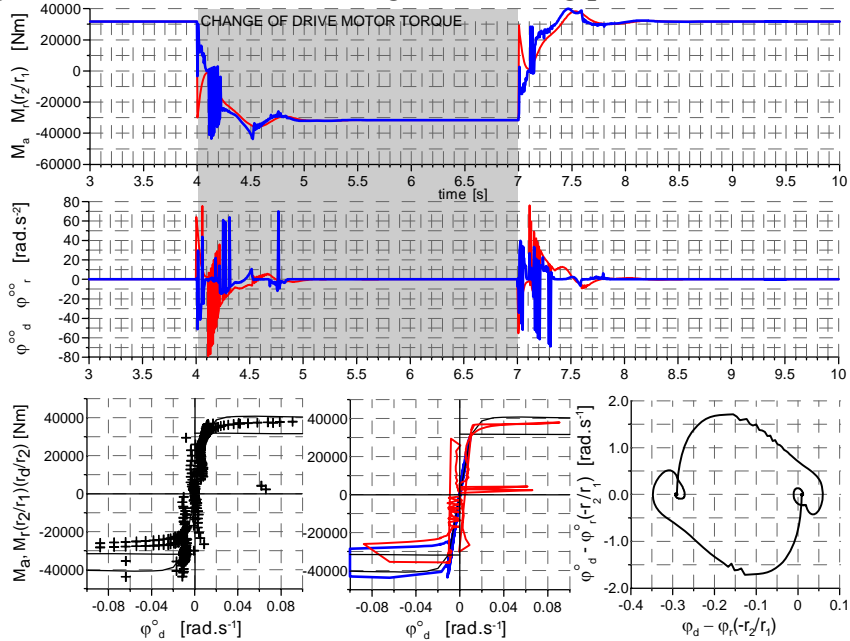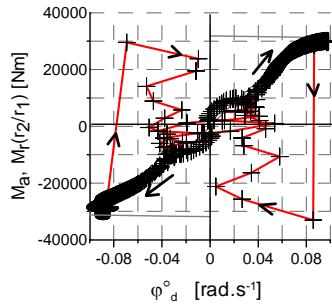

**Fig. 18 Transition action between traction work and dynamic braking**

Fig. 19 The zoom of bifurcation at interval $\dot{\varphi}_d$ (-0,1; 0,1)

The precision of torsional clearance of gear modelling has significant influence. According to [4] was used interpolation of linear binding characteristics by 6 degrees polynom, that has for this case the form:

$$M_{r1} = 148 - 83{,}7\mathrm{e}4 \cdot r_{r1} - 73{,}4\mathrm{e}6 \cdot r_{r1}^2 + 38{,}5\mathrm{e}10 \cdot r_{r1}^3 +$$
$$+ 86{,}32\mathrm{e}11 \cdot r_{r1}^4 - 86{,}82130\mathrm{e}14 \cdot r_{r1}^5 - 28{,}3406622\mathrm{e}16 \cdot r_{r1}^6$$

On the graphs at *fig. 20* we can see the effect of precision of binding modelling. The angular acceleration of rotor (as output from simulation calculation) is smaller abouth 20 rad.s^{-2} and more precisely convergence to reality.

Demonstration areas yourself requires the research in the field of simulation calculations and in the field of experimental research of braking adhesion characteristics, especially shape at field of braking according to UIC.
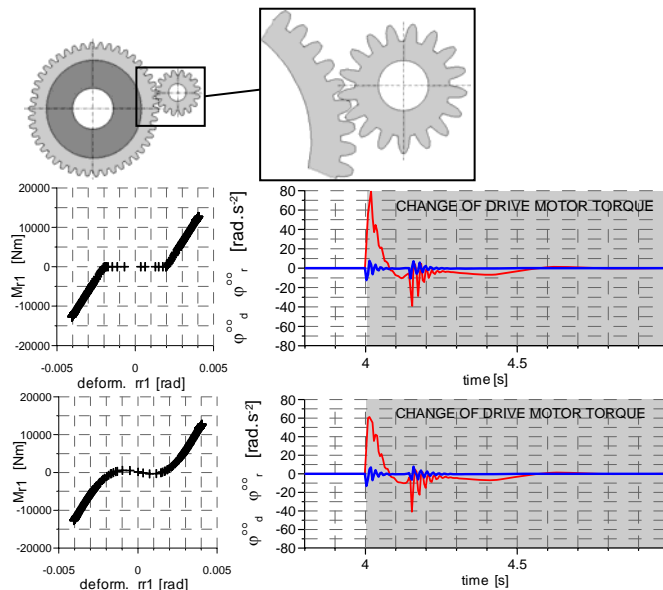
Fig. 20 The kinematic binding deformation and angular acceleration

This paper shortly shows dynamics torsional system simulation of railway drive vehicle. Most attention is given to the cooperation cases of adhesive characteristics with drive motor characteristics behind downgrade adhesive conditions they are simulation and influence on all system dynamics is analyzing. Full report knowledge of objective dynamic transitional phenomenon is necessary for solving of drive regulation and predicate the load of his main parts. Allow as well judge the dynamism influence on interaction with track if need be bring out the special cases of attrition. Successful with compile of algorithm which makes it possible judge the drive in a few

characteristic transitional actions. Make possible for example appreciation of reaction of system on changes input parameters. Make possible with behind go e.g. simulation slip-resistant regulation.

REFERENCES

[1] FREIBAUER, L. *Adheze kola na vozidlove draze. 7. ved. Konference VSDS,* Zilina 1983, s. 214-219.

[2] ČÁP, J. *Některé otázky vztahu třecí a adhezní charakteristiky ve styku kola s kolejnicí, Žel.technika* 2/88, s. 66-69

[3] POLÁCH, O. *Optimierung moderner Lok-Drehgestelle durch fahrzeugdynamische Systemanalyse. EI-Eisenbahningenieur (53),* 7/2002, s.50-57.

[4] MEZYK, A. *Analiza i ksztaltowanie cech dynamicznych napedów elektromechanicznych.* Wydawnictvo Politechniki Ślaskiej. Gliwice, Poland (2002). ISBN 83-7335-078-0.

[5] NOVÁK, J. *Elektromechanicke systemy v doprave a ve strojirenstvi.* CVUT Praha (2002).